



Evaluating the intensity of the 803-keV γ ray of ^{210}Po using a $4\pi\alpha\beta$ (LS)- γ (HPGe) measurement system

O. Aviv^{a,*}, S. Nissim^{a,b}, M. Brandis^a, Z. Yungrais^a, L. Weissman^a, A. Shor^a, E. Gilad^{b,**}

^a Soreq Nuclear Research Center, Yavne, 818000, Israel

^b Unit of Nuclear Engineering, Ben-Gurion University of the Negev, Beer-Sheva, 8410501, Israel

ARTICLE INFO

Keywords:

^{210}Po
HPGe detector
LSC
Gamma-ray spectrometry
Gamma-ray intensity

ABSTRACT

The absolute intensity for the 803-keV γ ray of ^{210}Po was evaluated by α - γ coincidence technique. A liquid sample with a known amount of ^{210}Po embedded in scintillation fluid was measured in a coincidence-based system that comprises a Liquid Scintillator (LS) detector and a High-Purity Germanium (HPGe) detector. A photo-reflector assembly that contains the ^{210}Po sample provides 100% efficiency for detecting the α particles. The combination between the HPGe and the LS detectors allows to reject non-coincident α - γ events while maintaining high resolution γ spectroscopy. Consequently, the faint 803-keV photopeak from ^{210}Po could be observed in a background-free environment, and its intensity could be evaluated with good accuracy. Sample measurements were carried out over nine months to gather statistics and verify the reliability of the experimental procedure. The absolute intensity of the 803-keV line was found to be $(1.22 \pm 0.03) \times 10^{-5}$, in excellent agreement with the adopted value in a recent data compilation and consistent with previous experimental works.

1. Introduction

Among the various radionuclides produced in the decay chains of the naturally occurring isotopes ^{238}U and ^{232}Th , ^{210}Po is considered to be of special interest due to its relatively high effective dose coefficient for inhalation (3.3×10^{-6} Sv/Bq) and ingestion (1.2×10^{-6} Sv/Bq) (IAEA, 2014). Following recommendations from various international organizations (e.g., World Health Organization), ^{210}Po is routinely monitored in the environment and particularly in drinking water in numerous countries (Grabowski and Bem, 2010; Landstetter et al., 2014; Matthews et al., 2007; Peck and Smith, 2000; WHO, 2018). Additionally, ^{210}Po plays an important role in research related to astrophysics where the cross section of the process $^{209}\text{Bi}(n, \gamma)^{210}\text{Bi}$ is studied via the decay $^{210}\text{Bi} \rightarrow ^{210}\text{Po}$ (Clayton and Rassbach, 1967). Therefore, accurate knowledge of the decay data of ^{210}Po is essential.

^{210}Po ($T_{1/2} = 138.4$ d) predominantly decays by α emission to the ground level of ^{206}Pb with an additional, weak branch for reaching an excited state of ^{206}Pb (Fig. 1). The transition from the excited to the ground state of ^{206}Pb is accompanied by one γ -ray emission (803 keV). Thus, identification and quantification of ^{210}Po in samples using a high-purity germanium (HPGe) detector can only be accomplished by

measuring the faint 803-keV emission. Although, determination of the activity concentration of ^{210}Po in drinking water is often performed by measuring α particles using silicon detectors and following extensive chemical procedures (to minimize contributions from other α emitters present in the original water sample) (IAEA, 2010).

The intensity of the 803-keV γ ray was evaluated mainly during the years 1951–1957 (Alburger and Pryce, 1954; Ascoli et al., 1956; Barber and Helm, 1952; Grace et al., 1951; Hayward et al., 1955; Ovechkin, 1957; Ovechkin and Tsenter, 1957; Riou, 1952; Rojo et al., 1955; Shmanskaja, 1957), and only two results were reported more recently (Ohtsuki et al., 1999; Shor et al., 2018). The absolute intensities for the 803-keV line appearing in two comprehensive nuclear libraries are $(1.23 \pm 0.04) \times 10^{-5}$ (Nucléide-Lara, 2022) and $(1.03 \pm 0.06) \times 10^{-5}$ (Kondev, 2008). Namely, the adopted literature values deviate from each other by 19%; therefore, additional measurements are needed to resolve this discrepancy.

One of the main challenges in evaluating the intensity of the 803-keV line is an insufficient sensitivity of common γ spectrometers for observing the corresponding photopeak as it is usually overwhelmed by events originating from background radiation. A typical experimental procedure for preparing a test sample involves the deposition of a thin

* Corresponding author.

** Corresponding author.

E-mail addresses: oferav@soreq.gov.il (O. Aviv), gilade@bgu.ac.il (E. Gilad).

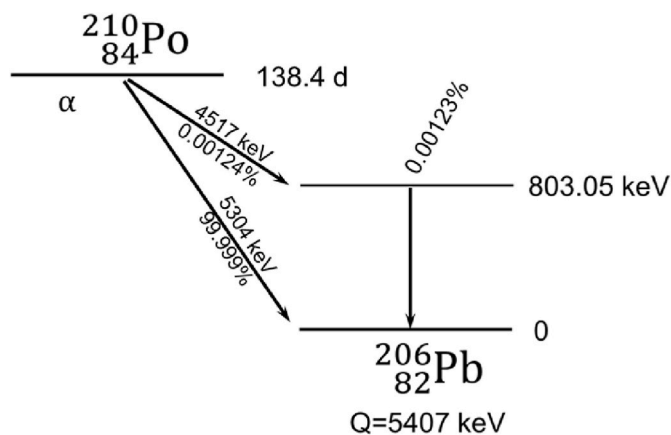


Fig. 1. Simplified decay diagram of ^{210}Po (Nucléide-Lara, 2022).

layer of high-purity ^{210}Po with high activity (0.1–10 GBq) onto a metal foil (Ascoli et al., 1956; Hayward et al., 1955; Ovechkin and Tsenter, 1957). The sample is then placed for measurements in separate systems that detect α and γ emissions. The uncertainty associated with past evaluations was within the range of 5–27% and mainly originated from detector calibrations, uncertainty of sample activity as well as counting statistics (Alburger and Pryce, 1954; Barber and Helm, 1952; Grace et al., 1951; Hayward et al., 1955; Ohtsuki et al., 1999; Ovechkin and Tsenter, 1957; Riou, 1952; Shimanskaia, 1957; Shor et al., 2018).

An alternative method for determining the absolute intensity of the 803-keV emission from ^{210}Po was developed, tested, and presented in this paper. A liquid sample of ^{210}Po with known activity was measured using a $4\pi\alpha\beta(\text{LS})-\gamma(\text{HPGe})$ system that enables simultaneous detection of α particles and γ rays. Data was recorded in listmode and analyzed offline. By employing a timing constraint between the detected α and γ from ^{210}Po , other events originating from the prominent transition (as well as from background radiation) can be rejected and the weak 803-keV photopeak can be observed practically undisturbed. The experimental procedure is described, and results are presented and discussed.

2. Materials and methods

2.1. Experimental setup

The experimental system, shown in Fig. 2 (left), consists of a mobile HPGe detector (model GC6022, Canberra) and a photo-multiplier tube (PMT), both facing a vial that contains the radioactive sample mixed with scintillation cocktail (Nissim et al., 2022, 2023). The HPGe detector exhibits a 58% relative detection efficiency compared to a $3'' \times 3''$ NaI (TI) detector and achieves a 2.0 keV resolution when measuring a γ -ray energy of 1332.5 keV. The assembly, comprising the PMT, a socket, and the vial, effectively serves as a liquid scintillation (LS) detector used to measure α and β particles. The socket is made of polylactic acid (PLA)

and coated with diffusive film for improved light transfer and is shown in Fig. 2 (right). Copper (1-cm thick) and lead (10-cm thick) are used to shield the detectors. Sheets of black polyethylene and a wood box (1-cm thick) that house the detectors and shielding materials provide a light-tight environment.

The output signals from the pre-amplifiers of HPGe and the LS detectors are connected to a digitizer (model DT5725, CAEN). The digitizer includes an amplifier, pulse shaper, multi-channel analyzer (16,384 channels) and analog-to-digital converter for each of its eight inputs as well as an internal clock (125 MHz). Two function generators (model PB4, BNC) are connected in sequence to the inputs of the pre-amplifiers to provide a continuous logic pulse for synchronization and assessment of the measurement live-time (in addition to that provided by the digitizer). Data acquisition and control over signal processing parameters are done by the CoPASS software (version 1.5.2) (CAEN, 2019).

2.2. ^{210}Po sample

An aliquot with 6060 ± 106 Bq of ^{210}Po (Eckert & Ziegler Analytics, USA) embedded in 10 ml of scintillation cocktail (UltimaGold™ AB, PerkinElmer) was supplied in a sealed 20-cc glass vial. No further preparation arrangements were required, and the sample was placed for measurements as is, thereby reducing potential safety risks related to sample handling.

2.3. Measurements and analysis

Repeated sample measurements were carried out over nine months to (a) gather satisfactory counting statistics; (b) compare the time dependency of the detected events from the ^{210}Po sample with its expected decay trend ($T_{1/2} = 138.4$ d); (c) study potential contributions of events originating from background signal or from contaminants that may be present in the sample. Throughout the experimental campaign, an identical geometrical configuration was used where the sample vial was fixed to the same position and in contact with both detectors (Fig. 2). In each measurement, the timestamp and energy were recorded event-by-event and for each detector. Analysis was performed offline using a dedicated set of software codes developed and ran in MATLAB™. True coincidence events were identified by requiring a timing difference of up to 700 ns between the HPGe and LS detectors. Spectra of the HPGe (γ) and LS (α/β) detectors were generated in both singles and coincidence modes. To further suppress contributions from background events, coincidence spectra of the HPGe detector were generated upon selecting events that correspond to α -particles (i.e. around 4.5 MeV) in the region of interest of the LS spectra. Likewise, LS spectra were generated upon selecting γ events in the region of interest of the HPGe spectra (i.e. around 803 keV). It is stressed that the net number of coincident events did not decrease when applying these spectrometric cuts.

The method for calculating the intensity of the 803-keV line is described hereafter. The general expression for the activity of an α emitter measured by a LS detector (singles mode) is given by (Knoll,

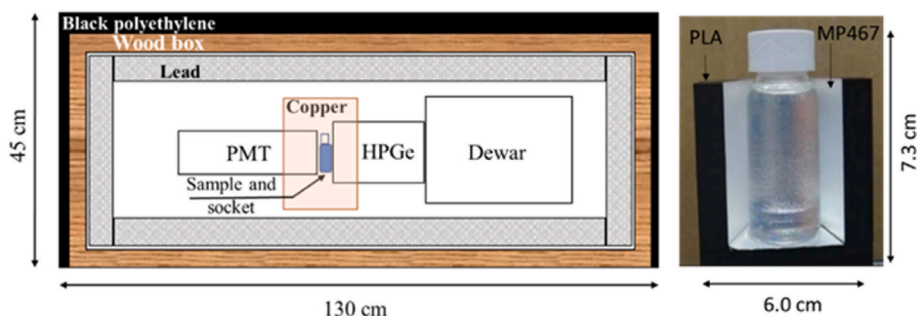


Fig. 2. Left: Side view of the $4\pi\alpha\beta(\text{LS})-\gamma(\text{HPGe})$ measurement system. Right: Front view of the reflective socket (Nissim et al., 2023).

2010):

$$A = \frac{N_{\alpha}^{sing}}{\tau_L^{sing} \bullet \epsilon_{\alpha} \bullet I_{\alpha} \bullet F_d} \quad (1)$$

where N_{α}^{sing} is the net α -peak counts, τ_L^{sing} is the measurement live-time of the LS detector, ϵ_{α} is the detection efficiency of the LS detector for α particles, and I_{α} is the emission intensity. F_d is the correction factor accounting for the decay during the measurement real time (t_R) and is given by $F_d = (1 - e^{-\lambda \bullet t_R}) / (\lambda \bullet t_R)$, where λ is the decay constant of the measured radionuclide. The general expression for the activity of a radionuclide measured by a HPGe detector (singles mode) is given by (Knoll, 2010):

$$A = \frac{N_{\gamma}^{sing}}{t_L^{sing} \bullet \epsilon_{\gamma} \bullet I_{\gamma} \bullet F_d} \quad (2)$$

where N_{γ}^{sing} is the net photopeak counts, t_L^{sing} is the measurement live-time of the HPGe detector, ϵ_{γ} is the detection efficiency of the HPGe detector for γ rays, and I_{γ} is the γ -ray intensity. Similarly, the activity of an α - γ emitter measured by the HPGe detector in coincidence with the LS detector can be expressed by:

$$A = \frac{N_{\gamma}^{coin}}{t_L^{coin} \bullet \epsilon_{\gamma} \bullet \epsilon_{\alpha(\gamma)} \bullet I_{\gamma} \bullet F_d} \quad (3)$$

where N_{γ}^{coin} and t_L^{coin} are the net photopeak counts and the measurement live-time in coincidence mode, respectively. $\epsilon_{\alpha(\gamma)}$ is the detection efficiency for an α particle which coincides with the γ ray. Based on Equations (1)–(3), it is possible to derive the intensity of the 803-keV γ ray from ^{210}Po with two approaches:

- (i) Using the known sample activity (decay corrected to the measurement time):

$$I_{\gamma} = \frac{N_{\gamma}^{coin}}{A \bullet t_L^{coin} \bullet \epsilon_{\gamma} \bullet \epsilon_{\alpha(\gamma)} \bullet F_d} \quad (4)$$

- (ii) Using the well-known intensity of the main α branch ($I_{\alpha} = 99.99876\%$):

$$I_{\gamma} = I_{\alpha} \frac{N_{\gamma}^{coin}}{N_{\alpha}^{sing}} \frac{1}{\epsilon_{\gamma}} \frac{\epsilon_{\alpha}}{\epsilon_{\alpha(\gamma)}} \frac{\tau_L^{sing}}{t_L^{coin}} \quad (5)$$

The detection efficiency of the system was established for α particles and γ rays using calibrated sources having identical geometry as the ^{210}Po sample (subsection 2.4). In addition, a blank sample (i.e. a vial containing only 20 ml of scintillation cocktail) was prepared and measured for seven days to evaluate potential background contributions in the regions of interest in spectra acquired by the HPGe and LS detectors (subsection 3.1).

2.4. Calibration

The detection efficiency of the HPGe detector for γ rays was determined using a mixed solution of radionuclides (^{241}Am , ^{139}Cd , ^{137}Cs , ^{109}Cd , ^{88}Y , ^{65}Zn , ^{60}Co , ^{57}Co , ^{54}Mn and ^{51}Cr) with known activity concentrations that cover the photon energy range of 59.5–1836.1 keV. A weight of 0.160 ± 0.001 g was extracted from a master solution (having certified activity concentrations) and injected into a 20-cc glass vial containing 9.84 g of carrier solution. This calibration source was measured in singles mode for 3 h. The dependence of the detection efficiency on the photon energy was established according to standard procedure (Knoll, 2010). Fig. 3 shows the determined detection efficiency together with the fitting function $\log(\epsilon_{\gamma}) = \sum_{i=0}^4 a_i \bullet E_{\gamma}^{i-1}$ (solid line). The Monte-Carlo software GESPECOR (Sima et al., 2001) was used

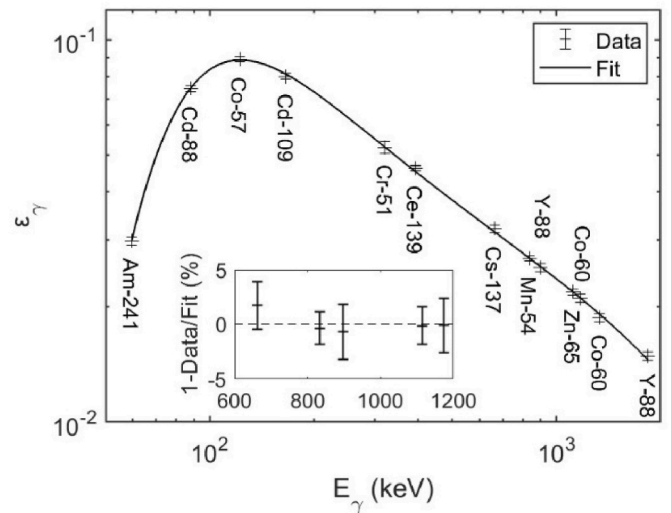


Fig. 3. Determined detection efficiency of the HPGe detector in singles mode together with a fit (solid line). The inset shows the relative difference between the data points and the fit in the energy range of 600–1200 keV.

to estimate the cascade summing corrections for ^{60}Co and ^{88}Y assuming approximate detector-sample geometry. Statistical uncertainties of the data points are typically 1% and the deviations from the fitted values are below 1% in the energy range of 800–900 keV (inset of Fig. 3), which is of interest for ^{210}Po . The adopted detection efficiency of the HPGe detector for 803-keV is 0.0276 ± 0.0005 .

By measuring an α - γ emitter in the system the efficiency of the LS detector for α particles can be established from the ratio between the rate of net photopeak counts in coincidence mode to that in singles mode (Cooper et al., 2013):

$$\epsilon_{\alpha} = \left(\frac{N_{\gamma}^{coin}}{t_L^{coin}} \right) \bigg/ \left(\frac{N_{\gamma}^{sing}}{t_L^{sing}} \right) \quad (6)$$

The radionuclide ^{226}Ra was selected for calibration as it emits an α particle with an energy of 4.8 MeV, similar to those emitted from ^{210}Po (Fig. 1). A weight of 0.0129 g (equivalent to 431 Bq) was extracted from a solution with a certified activity concentration of ^{226}Ra and injected into a glass vial containing 10 ml of scintillation cocktail (UltimaGold™ LLT, PerkinElmer). The spectral quenching parameter (SQP) of the prepared calibration source was evaluated by a commercial LS counter (model Quantulus GCT6220, PerkinElmer) and found to be ~ 650 and similar to that of the ^{210}Po sample (~ 700). Such a value for the SQP represents a negligible quenching effect (Piraner and Jones, 2020). The calibration source was measured for 20 h, thereby achieving a counting uncertainty of 0.6% in the 186-keV photopeak of ^{226}Ra . It is noted that the photopeak 186 keV also appeared in the blank measurement in singles mode (Fig. 4), therefore its relative contribution to the source counts (1%) was accounted for in the efficiency calculation. Thus, it was found that $\epsilon_{\alpha} = 1.000 \pm 0.015$, in a very good agreement with previous tests (Nissim et al., 2023) and as expected for liquid scintillation systems (Feng et al., 2017). The determined α -efficiency was adopted for the two α particles from ^{210}Po as their energies are very similar (Fig. 1).

3. Results

3.1. Blank measurement analysis

Fig. 4 shows a spectrum of a blank sample that was acquired for seven days by the HPGe detector (left) and LS detector (right) in both singles (black) and coincidence (blue) modes. The coincidence spectrum of the HPGe (LS) detector involves a spectrometric cut in the region of interest on the spectrum of the LS (HPGe) detector. Specifically, the

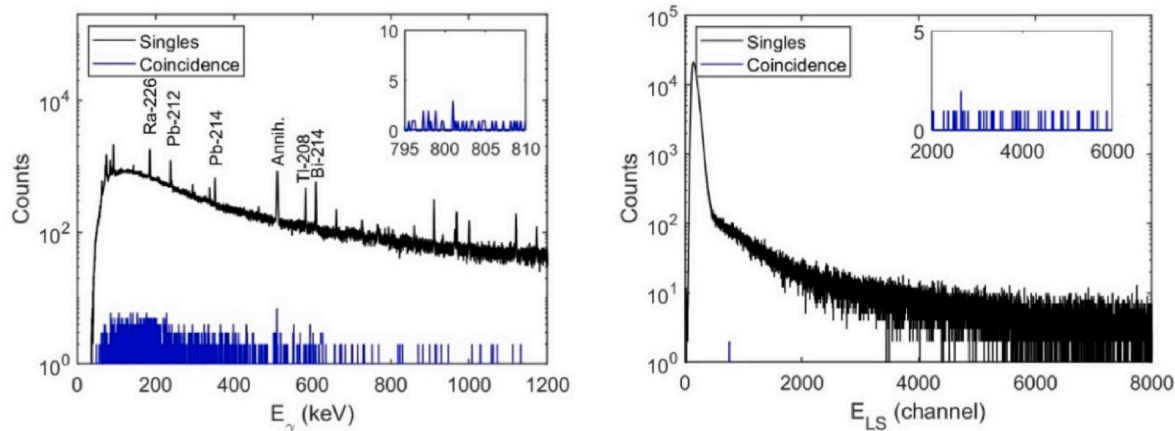


Fig. 4. Spectra of a blank sample measured for seven days by the HPGe detector (left) and LS detector (right) in singles (black) and coincidence (blue) modes. Coincidence spectra include spectrometric cuts. The insets show the regions of interest in coincidence mode. (For interpretation of the references to colour in this figure legend, the reader is referred to the web version of this article.)

region of interest in the HPGe spectrum is 795–810 keV, and the region of interest in the LS spectrum is channels 2000–6000 (see also Fig. 5). Common background photopeaks (e.g., 583.2 and 609.3 keV) as well as Compton scattering associated with radionuclides of natural origin (e.g., ^{208}Tl and ^{214}Bi) are observed in singles mode only. Similarly, the prominent peak appearing in the low channel range of the LS spectrum in singles mode (probably originating from electronic noise) was completely rejected in coincidence mode. The gross count rate in the region of interest of the HPGe spectrum was found to be $4 \times 10^{-5} \text{ s}^{-1}$ which is significantly lower than the expected γ event rate of $\sim 10^{-3} \text{ s}^{-1}$ from the ^{210}Po sample, considering the sample activity, the detection efficiency and the literature value for the γ -ray intensity (see Equation (2)). Similarly, the rate of background events in the region of interest of the LS detector is $5 \times 10^{-2} \text{ s}^{-1}$ which is considerably lower than the expected α event rate of $\sim 10^3 \text{ s}^{-1}$ from the ^{210}Po sample (see Equation (1)). In conclusion, it was demonstrated that the $4\pi\alpha\beta(\text{LS})-\gamma(\text{HPGe})$ system is effective in rejecting events originating from background radiation and provides sufficient sensitivity for conducting this experiment, as predicted for coincidence-based systems (Grigorescu, 1996).

3.2. ^{210}Po sample measurements

Table 1 shows the details of the measurements of the ^{210}Po sample.

Table 1

Details of the measurements of the ^{210}Po sample. Uncertainties are given at a confidence level of 1σ .

Run number	Time since reference date (d)	Duration (d)	$N_{\alpha}^{\text{sing}} (\times 10^9)$	N_{γ}^{coin}
1	18	6.8	2.941 ± 0.001	950 ± 35
2	33	5.5	2.204 ± 0.001	758 ± 31
3	45	6.3	2.384 ± 0.001	781 ± 33
4	53	4.8	1.748 ± 0.001	573 ± 24
5	59	6.5	2.316 ± 0.001	777 ± 31
6	67	6.0	2.063 ± 0.001	741 ± 30
7	73	6.5	2.170 ± 0.001	702 ± 29
8	172	1.9	0.411 ± 0.001	136 ± 17
9	192	2.5	0.479 ± 0.001	168 ± 18
10	220	3.5	0.584 ± 0.001	198 ± 26
11	269	3.0	0.395 ± 0.001	138 ± 21
12	294	3.8	0.442 ± 0.001	148 ± 26

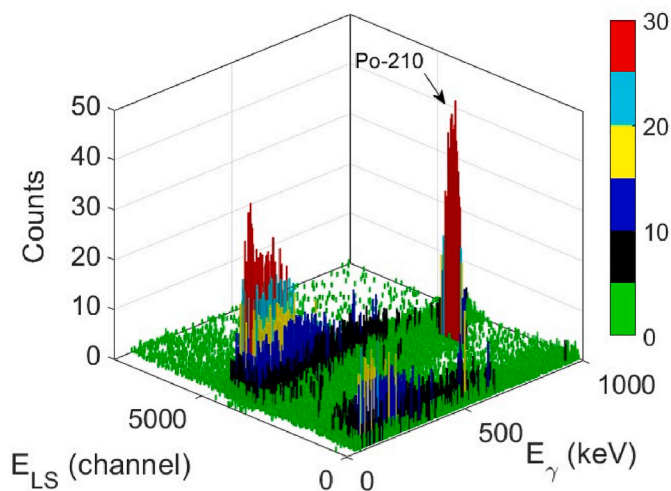


Fig. 5. 2D α - γ coincidence spectrum of the ^{210}Po sample measured during 7 d (run #1, Table 1).

Altogether 12 individual measurements were performed over nine months. The total measurement duration was 57 d, where each run was performed between 2 d and up to 7 d. The elapsed times between the reference date of the certified activity and measurement start times ranged from 18 d and up to 294 d. Data was recorded in both singles and coincidence modes for the HPGe and LS detectors. The net counts of α particles (singles mode) and coincident α - γ are presented in Table 1. The decay correction factor F_d was calculated for each run, being 0.982–0.995 (depending on the measurement duration). The accumulated net counts for N_{α}^{sing} and N_{γ}^{coin} was found to be 1.81×10^{10} and 6070, respectively. The counting uncertainty for each run was found to be typically $<0.1\%$ for N_{α}^{sing} and 4–15% for N_{γ}^{coin} , depending on the measurement duration and sample's age. As expected, the dead time of the HPGe detector (singles mode) was $<0.5\%$, given the low γ -emission rate from the sample (see also Fig. 6 (left)). In comparison, the dead time of the LS detector during measurements was 2–9% (depending on the sample age) due to the high count-rate of α particles (i.e. 2000–6000

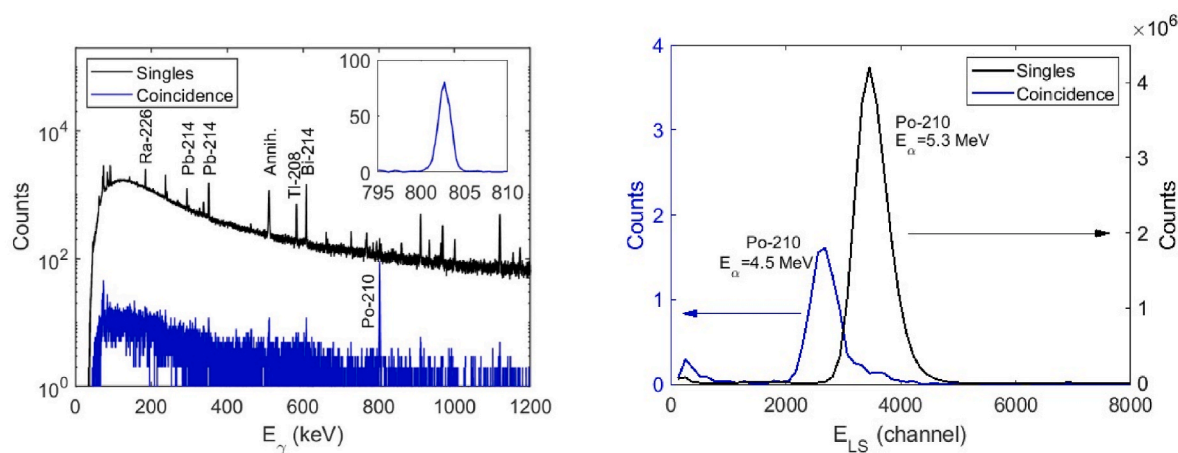


Fig. 6. Spectra of ^{210}Po sample measured for 7 d in singles (black) and coincidence (blue) modes in the HPGe detector (left) and LS detector (right). Coincidence spectra include spectrometric cuts. LS spectra are binned for visualization. (For interpretation of the references to colour in this figure legend, the reader is referred to the web version of this article.)

s^{-1}). Thus, the effective live time in coincidence mode was that of the LS detector in singles mode (i.e. $t_L^{\text{coin}} \approx \tau_L^{\text{sing}}$). When also considering that $\varepsilon_\alpha = 1$ and $I_\alpha \approx 1$, Equation (5) which is used for calculating the 803-keV intensity according to approach (ii), can be simplified to

$$I_\gamma = N_\gamma^{\text{coin}} / N_\alpha^{\text{sing}} / \varepsilon_\gamma \quad (7)$$

Runs #1, #11 and #12 were performed without applying the pulser (see subsection 2.1), and their corresponding live times were retrieved from the data acquisition software. For consistency in the analysis, the data from these runs was used only in approach (ii) as it is independent on the measurement time.

Fig. 5 shows an example for a two-dimensional coincidence spectrum of the sample. The prominent peak at $E_\gamma = 803$ keV (with the corresponding channel of ~ 3000 in the LS detector) originates from the weak γ emission of ^{210}Po . Peaks within the low photon energy range of 72–87 keV (with the corresponding channel of ~ 3800 in the LS detector) probably originate from the very weak ($\sim 10^{-6}\%$) x-rays emitted from ^{206}Pb following the α decay (Fischbeck and Freedman, 1975; Nucléide-Lara, 2022). Other events mostly appearing in the low photon energies may originate from electronic noise and/or random coincidence. As shown in Fig. 5, the 803-keV photopeak is well separated from other events in the spectrum, and its area can be determined reliably.

Fig. 6 (left) shows the γ spectrum from run #1 (Table 1) in singles (black) and coincidence (blue) modes. The coincidence spectra of the HPGe (LS) detector include an energy cut on the corresponding region of interest in the spectrum of the LS (HPGe) detector (see also Fig. 5). The γ -singles spectrum shows the usual photopeaks associated with background radiation and is practically identical to the spectrum of the blank sample measurement (Fig. 4 (left)). In comparison to the high level of continuum counts observed in singles mode, the γ spectrum in coincidence mode exhibits a prominent peak at 803 keV (inset of Fig. 6 (left)). No other photopeaks were observed that could indicate the presence of radioactive contaminants in the ^{210}Po sample.

Fig. 6 (right) shows the LS spectrum from run #1 in both singles (black) and coincidence (blue) modes. The prominent peaks in singles mode and coincidence mode correspond to the main (5.3 MeV) and weak (4.5 MeV) α emission from ^{210}Po (Fig. 1), respectively. As expected, events arising from the ^{210}Po sample are significantly larger than any background signal in singles mode (see also Fig. 4 (right)), where counts on both sides of the 5.3-MeV peak are lower by a factor of $\sim 10^3$ than those within the α -peak. Thus, it was demonstrated that the $4\pi\alpha\beta$ (LS)- γ (HPGe) system can discriminate between the two α -decays of ^{210}Po (Fig. 1).

As a consistency check for the overall experimental procedure, trends

of the measured counts were compared to the expected decay of ^{210}Po . Fig. 7 shows the determined count rates from all runs (Table 1) in singles (left) and coincidence (right) modes. The solid lines in Fig. 7 represent exponential fits using the literature decay constant of ^{210}Po , namely $\lambda = 5.798 \times 10^{-8} \text{ s}^{-1}$. A very good agreement was observed between the data points and the expected decay trends ($R^2 > 0.99$). In addition, the fitted value at $t = 0$ for the detected α count rate in singles mode was found to be $6105 \pm 20 \text{ s}^{-1}$ (Fig. 7 (left)). This value translates to an initial activity of 6105 Bq (see Equation (1)) when considering the literature intensity of nearly 100% for the main decay branch and the system's 100% efficiency for detecting α particles (see subsection 2.4). This result for the initial activity is in excellent agreement with the certified sample activity (i.e. $6060 \pm 106 \text{ Bq}$).

3.3. Emission intensity evaluation

The entire dataset (Table 1) was used to determine the intensity of the 803-keV line using approaches (i) and (ii), described in subsection 2.3. Results are presented in Table 2. The calculated intensity and its uncertainty for both approaches were determined from the weighted mean value where common systematic uncertainties (e.g., detection efficiencies) were added separately (see also Table 3). The determined values from both approaches were found to be in excellent agreement.

The uncertainty budget for both approaches is presented in Table 3. While approach (i) provides a combined uncertainty of 3.5%, approach (ii) provides an even better uncertainty of 2.5%. The main contributing parameters to the uncertainty in approach (i) include sample activity, counting statistics as well as detection efficiencies. Furthermore, the uncertainty in approach (ii) mainly originates from the determined detection efficiency for the 803-keV γ ray and counting statistics (see also subsections 2.3, 2.4 and 3.2). Thus, it should be possible to further improve the overall uncertainty by increasing the counting statistics, which can be accomplished by using a sample with larger activity and performing longer measurements. In summary, the intensity of the 803-keV γ ray was determined by averaging the results from both approaches, namely $I_{803} = (1.22 \pm 0.03) \times 10^{-5}$.

Fig. 8 shows the reported intensity for the 803-keV line of ^{210}Po from several works. Thus, the determined value from this work is in very good agreement with experiments performed within 1955–1957 and the adopted literature value of $(1.23 \pm 0.04) \times 10^{-5}$ (Nucléide-Lara, 2022), and consistent with the most recent work (Shor et al., 2018). In addition, the uncertainty achieved by the present method is lower than those from other well-established experimental procedures.

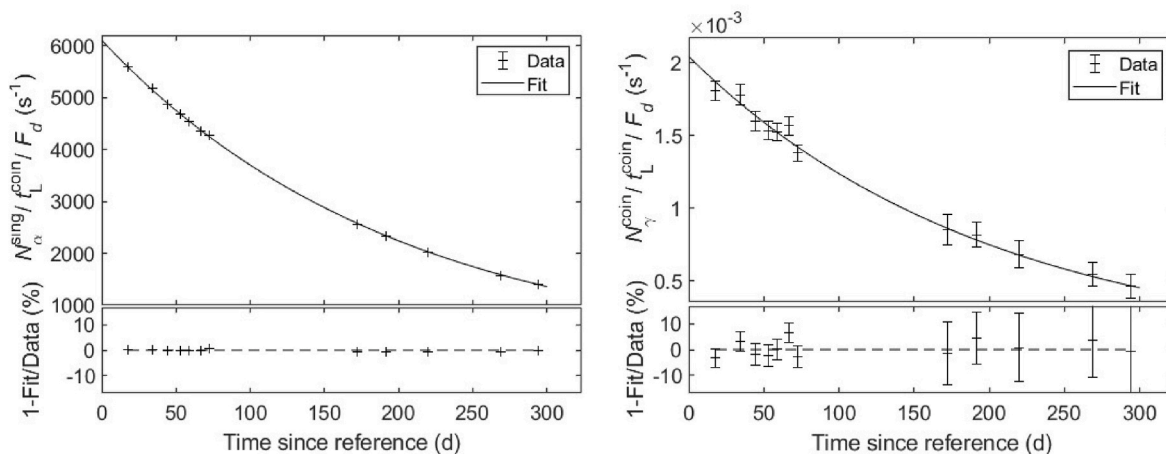


Fig. 7. Top: Net peak count rates (corrected for decay during measurement) in singles (left) and coincidence (right) mode from the measured ^{210}Po sample since its reference time. The solid lines denote exponential fits using the literature value of the decay constant for ^{210}Po . Bottom: Relative differences between the data points and the fits.

Table 2

Determined absolute intensity of the 803-keV γ ray from ^{210}Po . Uncertainties are given at a confidence level of 1σ .

	Approach (i)	Approach (ii)
I_{803}	$(1.226 \pm 0.043) \times 10^{-5}$	$(1.209 \pm 0.031) \times 10^{-5}$

Table 3

Uncertainty budget for approaches (i) and (ii).

Parameter	Symbol	Assigned uncertainty (1σ)	
		Approach (i)	Approach (ii)
Sample activity	A	1.7%	–
Detection efficiency for γ	ϵ_γ	2.0%	2.0%
Detection efficiency for α	ϵ_α	1.5%	–
Net γ counts	N_γ^{coin}	1.7%	1.5%
Net α counts	N_α^{sing}	–	<0.1%
Decay constant	λ	<0.1%	–
Decay correction	F_d	0.1%	–
Intensity of the main α branch	I_α	–	<0.1%
Live time	t_L	0.5%	<0.1%
Combined uncertainty		3.5%	2.5%

4. Summary and conclusions

A new measurement of the intensity for the faint 803-keV γ ray emitted from ^{210}Po was performed using a $4\pi\alpha\beta(\text{LS})-\gamma(\text{HPGe})$ system. A liquid sample of ^{210}Po embedded in a scintillation cocktail was placed for measurement. The experimental system, comprising a HPGe detector coupled to a LS detector, was used to detect coincident α particle and γ ray originating from ^{210}Po , thereby allowing to observe the 803-keV photopeak practically undisturbed. The intensity of the 803-keV line was evaluated using two approaches; the first relied on the known sample activity, and the second relied on the well-known intensity of the main α -emission from ^{210}Po . The absolute intensity from both approaches was $(1.22 \pm 0.03) \times 10^{-5}$, in very good agreement with the adopted value appearing in a recently published nuclear decay database. In addition, the low uncertainty obtained in this work is competitive to those from previous experiments. The main advantages of the presented method include a relatively simple and safe procedure for conducting the measurement, a good signal-to-noise ratio, and a low uncertainty. The method and experimental system described in this work can be extended to other case studies, where certain branching ratios of relatively short-lived (days-weeks) radionuclides decaying by α - γ emission

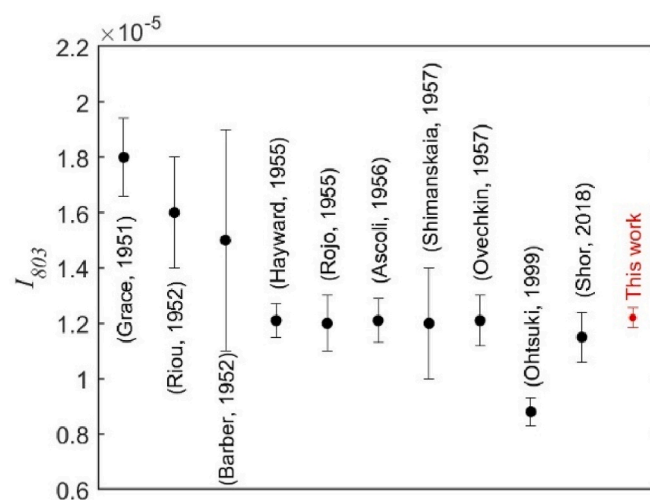


Fig. 8. Result for the absolute intensity of the 803-keV γ ray of ^{210}Po from previous experiments and the present work.

can be determined with high accuracy.

CRediT authorship contribution statement

O. Aviv: Writing – original draft, Visualization, Supervision, Methodology, Formal analysis, Conceptualization. **S. Nissim:** Writing – original draft, Formal analysis, Data curation, Conceptualization. **M. Brandis:** Writing – original draft, Visualization, Supervision, Resources, Methodology, Investigation. **Z. Yungrais:** Resources, Project administration. **L. Weissman:** Writing – review & editing, Writing – original draft, Methodology, Conceptualization. **A. Shor:** Writing – review & editing. **E. Gilad:** Writing – review & editing, Supervision.

Declaration of competing interest

The authors declare that they have no known competing financial interests or personal relationships that could have appeared to influence the work reported in this paper.

Data availability

Data will be made available on request.

References

- Alburger, D., Pryce, M., 1954. Energy levels in Pb^{206} from the decay of Bi^{206} . *Phys. Rev.* 95, 1482–1499.
- Ascoli, A., Asdente, M., Germagnoli, E., 1956. On the ratio between γ - and α -activities in ^{210}Po . *Il Nuovo Cimento* 4, 946–947.
- Barber, W., Helm, R., 1952. Evidence for K-shell ionization accompanying the alpha-decay of Po^{210} . *Phys. Rev.* 86, 275–280.
- CAEN, 2019. User Manual UM5960 COMPASS - Multiparametric DAQ Software for Physics Applications. CAEN Electronic Instrumentation.
- Clayton, D.D., Rassbach, M., 1967. Termination of the s-process. *Astrophys. J.* 148, 69–85.
- Cooper, M.W., Ely, J.H., Haas, D.A., Hayes, J.C., McIntyre, J.I., Lidey, L.S., Schrom, B.T., 2013. Absolute efficiency calibration of a beta-gamma detector. *IEEE Trans. Nucl. Sci.* 60, 676–680.
- Feng, X.-g., Jiang, G.-h., Huang, J.-h., Du, J.-y., He, Q.-g., Wang, J.-c., Chen, J., Liu, X.-g., 2017. A performance comparison of two kinds of liquid scintillation counters from PerkinElmer, Inc. *J. Radioanal. Nucl. Chem.* 314, 629–635.
- Fischbeck, H.J., Freedman, M.S., 1975. Spectroscopy of α and K- and L-electron continua and L-electron pickup in ^{210}Po α decay. *Phys. Rev. Lett.* 34, 173–176.
- Grabowski, P., Bem, H., 2010. Determination of ^{210}Po and uranium in high salinity water samples. *J. Radioanal. Nucl. Chem.* 286, 455–460.
- Grace, M., Allen, R., West, D., Halban, H., 1951. Investigation of the γ -rays from polonium. *Proc. Phys. Soc.* 64, 493–507.
- Grigorescu, E.L., 1996. Low level gamma-spectrometry by beta coincidence. *Nucl. Instrum. Methods Phys. Res.* 369, 574–577.
- Hayward, R., Hoppes, D., Mann, W., 1955. Branching ratio in the decay of polonium-210. *J. Res. Natl. Bur. Stand.* 54, 47–50.
- IAEA, 2010. International Atomic Energy Agency (IAEA). A Procedure for Determination of Po-210 in Water Samples by Alpha Spectrometry.
- IAEA, 2014. International Atomic Energy Agency (IAEA). Radiation Protection and Safety of Radiation Sources: International Basic Safety Standards. General Safety Requirements (GSR) Part 3.
- Knoll, G.F., 2010. *Radiation Detection and Measurement*, fourth ed. John Wiley & Sons, New York, USA.
- Kondev, F., 2008. Nuclear data sheets for $A = 206$. *Nucl. Data Sheets* 109, 1527–1654.
- Landstetter, C., Hiegesberger, B., Sinojmeri, M., Katzlberger, C., 2014. Determination of ^{210}Pb and ^{210}Po in water using the extractive scintillation cocktail PoLex. *Appl. Radiat. Isot.* 93, 76–81.
- Matthews, K.M., Kim, C.-K., Martin, P., 2007. Determination of ^{210}Po in environmental materials: a review of analytical methodology. *Appl. Radiat. Isot.* 65, 267–279.
- Nissim, S., Brandis, M., Aviv, O., Arazi, L., 2023. Characterization of a $4\pi\alpha\beta$ (LS)- γ (HPGe) prototype system for low background measurements. *Appl. Radiat. Isot.*, 110866 (in press).
- Nissim, S., Aviv, O., Brandis, M., Weissman, L., Sasson, R., Yungrais, Z., Datz, H., Arazi, L., 2022. Evaluating the intensity of the 'prompt' 140.5 keV γ -ray of ^{99}Mo using a $4\pi\alpha\beta$ (LS)- γ (HPGe) measurement system. *Appl. Radiat. Isot.* 188, 110367.
- Nucléide-Lara, 2022. Laboratoire national henri becquerel (LNHB), nuclear and atomic data. Available online at: <http://www.nucleide.org/Laraweb>. . December 2022.
- Ohtsuki, T., Kasagi, J., Kasajima, N., Yamazaki, H., Yuki, H., Yukishima, M., 1999. Bremsstrahlung emission in α -decay of ^{210}Po . *J. Radioanal. Nucl. Chem.* 239, 123–126.
- Ovechkin, V., 1957. On the relative intensity of Po^{210} γ quanta. *Izvest. Akad. Nauk. SSSR* 21.
- Ovechkin, V.V., Tsenter, E.M., 1957. K ionization in α -decay of Po^{210} . *The Soviet Journal of Atomic Energy* 2, 344–348.
- Peck, G.A., Smith, J.D., 2000. Determination of ^{210}Po and ^{210}Pb in rainwater using measurement of ^{210}Po and ^{210}Bi . *Anal. Chim. Acta* 422, 113–120.
- Piraner, O., Jones, R.L., 2020. The effect of quench agent on urine bioassay for various radionuclides using QuantulusTM1220 and Tri-CarbTM3110. *J. Radioanal. Chem.* 326, 657–663.
- Riou, M., 1952. Sur les rayonnements γ et x émis par le polonium 210. *Journal of Physical Radium* 13, 244.
- Rojó, O., Hakeem, M., Goodrich, M., 1955. Relative number of gamma-rays from Po-210. *Phys. Rev.* 99, 1629.
- Shimanskaia, N.S., 1957. *Sov. Phys. - JETP* 4, 165.
- Shor, A., Weissman, L., Aviv, O., Eisen, Y., Brandis, M., Paul, M., Plompen, A., Tessler, M., Vaintraub, S., 2018. Branching ratio to the 803 keV level in ^{210}Po α decay. *Phys. Rev. C* 97, 034303.
- Sima, O., Arnold, D., Dovlete, C., 2001. GESPECOR: a versatile tool in gamma-ray spectrometry. *J. Radioanal. Nucl. Chem.* 248, 359–364.
- WHO, 2018. World Health Organization (WHO). Management of Radioactivity in Drinking-Water.